

Diagnosing the AGN population origin of TeV neutrinos with their spatial correlation

XIAO-BIN CHEN,^{1,2} RUO-YU LIU,^{1,2,3} AND XIANG-YU WANG^{1,2,3}

¹*School of Astronomy and Space Science, Nanjing University, Nanjing 210023, China*

²*Key laboratory of Modern Astronomy and Astrophysics (Nanjing University), Ministry of Education, Nanjing 210023, China*

³*Tianfu Cosmic Ray Research Center, Chengdu 610000, Sichuan, China*

ABSTRACT

The recent IceCube detection of TeV neutrinos from some nearby Seyfert galaxy (e.g., NGC 1068) suggests that active galactic nuclei (AGN) could make a significant contribution to the diffuse flux of astrophysical neutrinos. The absence of TeV gamma-rays from NGC 1068 indicates neutrino production in compact gamma-ray-opaque region. The vicinity of the supermassive black hole, such as disk-corona, is an ideal region, where the high radiation density leads to efficient neutrino production as well as the gamma-ray attenuation. Disk-corona models predict that the neutrino emission from AGNs correlates with X-ray emission, which traces the coronal activity. In this paper, we assess whether the X-ray AGN population origin for TeV neutrinos can be tested by using the spatial correlation between the neutrino population and X-ray AGN population with future neutrino telescopes. By performing simulations, we find that, the AGN origin of the neutrino background above 100 TeV can be tested at a confidence level of $\sim 2.4\sigma$ with five-year observations of IceCube-Gen2, which has an angular resolution of ~ 0.2 degree. With better angular resolution and sensitivity in the energy range of above 300 TeV, a 30-km³ underwater neutrino telescope, such as High-energy Underwater Neutrino Telescope (HUNT), is expected to reach a significance of $\sim 8.6\sigma$ in testing the association after five years of exposure.

1. INTRODUCTION

The IceCube neutrino telescope has detected a significant number of neutrinos with energies between a few TeV and a few PeV. Searches for point-like sources associated with known astrophysical objects have largely returned null detection (M. G. Aartsen et al. 2020a), suggesting that the high-energy neutrino sky is dominated by an isotropic background. Although the origins of the vast majority of high-energy neutrinos have not been identified, a significant excess coming from the close-by Seyfert galaxy NGC 1068 at 4.2σ level (IceCube Collaboration et al. 2022) has been reported recently. Tentative excesses at 3σ level have also been reported from some other NGC 1068-like AGNs such as NGC 7469 and NGC 4151 (R. Abbasi et al. 2025a), implying that Seyfert galaxies could be common sources of high-energy neutrinos.

The neutrino flux measured from NGC 1068 is more than an order of magnitude larger than the upper limits of TeV gamma-ray emission placed by MAGIC and HAWC (V. A. Acciari et al. 2019; E. Wilcox & HAWC Collaboration 2022). The difference between the observed neutrino flux and gamma-ray flux from NGC 1068 suggests that the neutrinos must be produced in a region that is opaque to GeV–TeV gamma-

rays that would otherwise accompany the neutrinos. In Seyfert galaxies like NGC 1068, a hot and magnetized corona above the disk is formed (see e.g. K. A. Miller & J. M. Stone 2000). The dense environments near the supermassive black holes together with the acceleration of cosmic rays (CRs) in the corona offer suitable conditions for the production of high energy neutrinos. Such a scenario, commonly referred to as disk-corona models, has been shown to be able to accommodate the high level of neutrino emission from the X-ray bright AGN NGC 1068 (K. Murase et al. 2020; Y. Inoue et al. 2020; A. Kheirandish et al. 2021; B. Eichmann et al. 2022).

The large flux contrast between neutrinos and gamma rays in NGC 1068 is in agreement with the picture of gamma-ray “hidden” sources for the origin of the isotropic neutrino background (N. Senno et al. 2015; K. Murase et al. 2016; K. Bechtol et al. 2017; A. Capanema et al. 2020; K. Fang et al. 2022), as required by comparison of isotropic diffusive neutrino flux measured by IceCube (M. G. Aartsen et al. 2020b; R. Abbasi et al. 2022) and the isotropic gamma-ray background observed by Fermi-LAT (M. Ackermann et al. 2015). This consistency further supports the main contributors of the neutrino background are “hidden” sources. Building on this framework, D. F. G. Fiorillo et al. (2025) extended the NGC 1068 result to a population study

of X-ray-emitting AGNs and constructed an AGN luminosity sequence, demonstrating that the cumulative neutrino emission from such sources can account for the diffuse neutrino background observed by IceCube in the 1–100 TeV energy range.

However, the limited angular resolution and statistics of current IceCube data make it difficult to establish a significant spatial correlation between neutrinos and the population of X-ray AGNs. Previous searches by the IceCube Collaboration have mainly relied on stacking analyses that combine the likelihood contributions from multiple candidate sources (e.g. B. Zhou et al. 2021; R. Abbasi et al. 2023, 2025b), but no significant excess has yet been found so far. Future neutrino telescopes, such as IceCube-Gen2 (M. G. Aartsen et al. 2021), KM3NeT (S. Adrián-Martínez et al. 2016), Huge Underwater high-energy Neutrino Telescope (HUNT) (T. Q. Huang et al. 2024), Tropical Deep-sea Neutrino Telescope (TRIDENT) (Z. P. Ye et al. 2023), NEON (H. Zhang et al. 2025) and Baikal-GVD (I. Belolaptikov et al. 2022), will have larger effective volumes and improved angular precision, and are therefore crucial for testing this connection. Motivated by this, in this work we present a cross-correlation analysis to test the X-ray AGN population origin of TeV-PeV neutrinos with future neutrino telescopes. We will use IceCube-Gen2 and HUNT as two examples for the analyses. We assume the neutrino luminosity to be positively related to the X-ray luminosity of the AGN, given that the X-ray luminosity may reflect the energy production rate in the corona, and is also proportional to the target density for photopion production. By combining the AGN X-ray luminosity distribution with the expected performance of future neutrino telescopes, we forecast the prospects for detecting such a AGN-neutrino correlation.

2. SIMULATING NEUTRINO-AGN ASSOCIATIONS: MODELS AND METHODOLOGY

We evaluate the spatial correlation between high-energy neutrinos and AGNs by comparing how well the observed neutrino directions agree with the expectations under two competing scenarios for their astrophysical origins:

1. **AGN Association Hypothesis:** A subset or all of the detected neutrinos originate from AGNs, with their flux scaling proportionally to the X-ray fluxes of AGNs. In this scenario, the X-ray flux of an AGN serves as the proxy for its neutrino flux, reflecting the case in which AGNs are genuine neutrino emitters.

2. Null Hypothesis (Random Background):

Neutrino events are uncorrelated with AGNs and are isotropically distributed. Any apparent spatial association between AGNs and neutrinos arises purely by coincidence.

In both models, we account for contamination from atmospheric neutrinos, which form an irreducible background in high-energy neutrino observations. According to the IceCube 9.5-year dataset (R. Abbasi et al. 2022), the astrophysical signal starts to dominate the atmospheric neutrinos from 100 TeV (R. Abbasi et al. 2022).

The AGN catalog from the eROSITA Final Equatorial-Depth Survey (eFEDS) (T. Liu et al. 2022) forms the basis of our analysis. It includes 22,079 AGNs selected by X-rays in a contiguous 142 deg² field, with fluxes measured in the 0.2 – 2.3 keV band. Given its depth and well-characterized selection, the eFEDS sample provides a representative snapshot of the AGN population accessible to current wide-field X-ray surveys. Under the AGN-association hypothesis, we normalize the simulation by requiring that the total number of modeling neutrinos equals the expected number derived from the measured diffuse astrophysical neutrino flux plus the atmospheric neutrino background. These fluxes, taken from muon-neutrino flux with 9.5 years of IceCube data (R. Abbasi et al. 2022), are integrated over the chosen energy threshold and then folded with the effective area of the detector to yield the expected total count of events N_ν^{tot} . We assume that a fixed fraction f of these events is assigned to originate from AGNs, while the remainder is drawn from an isotropic atmospheric background. The parameter f denotes the fraction of astrophysical neutrinos with energies above a given threshold relative to the total neutrino population. The probability of each AGN producing a neutrino is taken to be proportional to its X-ray flux (F_X), i.e., $P_i \propto F_{X,i}$, ensuring that the sum of all AGNs reproduces $f \cdot N_\nu^{\text{tot}}$. For each AGN-origin neutrino assigned, its arrival direction is offset from the source position according to a two-dimensional Gaussian with a width equal to the detector’s point-spread function (PSF). In contrast, under the null hypothesis, neutrino positions are randomly drawn from a uniform distribution across the same sky footprint, with no relation with AGN locations.

3. UNBINNED LIKELIHOOD FRAMEWORK FOR SPATIAL CORRELATION ANALYSIS

3.1. Likelihood Method

An unbinned likelihood ratio method can be used to distinguish astrophysical neutrinos from the atmospheric background produced by cosmic ray interactions (J. Braun et al. 2008; C. Creque-Sarbinowski et al. 2022;

R. Abbasi et al. 2024). The optimal estimator to determine the fraction f of neutrinos associated with AGN is obtained using the unbinned maximum likelihood (ML) approach, formulated as

$$\mathcal{L}(f) = \prod_{i=1}^N [f \cdot S_i + (1 - f) \cdot B_i], \quad (1)$$

where S_i and B_i represent the signal and background probability density functions (PDFs), respectively, for the i -th neutrino event. The signal PDF S_i represents the likelihood of the i -th neutrino originating from the AGN population, modeled as a weighted sum over all AGNs in the field:

$$S_i = \sum_{\alpha} w_{\alpha} \frac{1}{2\pi\sigma_{\text{psf}}^2} \exp\left(-\frac{(\vec{x}_i - \vec{x}_{\alpha})^2}{2\sigma_{\text{psf}}^2}\right), \quad (2)$$

where \vec{x}_i and \vec{x}_{α} are the reconstructed positions of the neutrino and the α -th AGN, respectively, and $w_{\alpha} = F_{\alpha} / \sum_k F_k$ reflects the X-ray flux-weighted contribution of each AGN. Here F_{α} denotes the observed X-ray flux of the α -th AGN in the 0.2–2.3 keV band, as reported in the eFEDS catalog. The parameter σ characterizes the angular resolution (i.e. PSF) of the neutrino detector. The background PDF B_i accounts for neutrinos arising from the isotropic atmospheric background and is modeled as a uniform distribution over the analysis region: $B_i = \frac{1}{\Omega}$, where Ω is the solid angle subtended by the sky region covered by the AGN catalog and neutrinos.

The signal fraction f is determined by maximizing the likelihood function $\mathcal{L}(f)$ constructed over all observed neutrino events. Under the null hypothesis (i.e., no AGN contribution), the likelihood reduces to $\mathcal{L}(f = 0) = \prod_{i=1}^N B_i$. The strength of the signal is then quantified by the likelihood ratio test statistic:

$$\text{TS} = \lambda = -2 \cdot \log \left[\frac{\mathcal{L}(f)}{\mathcal{L}(f = 0)} \right], \quad (3)$$

which measures the relative preference for a nonzero f over the null hypothesis. To assess the uncertainty and confidence level on f , we define the signal-to-noise ratio as

$$\frac{S}{N_f} \equiv \frac{\hat{f}}{\sigma_f}, \quad (4)$$

where \hat{f} is the maximum-likelihood estimate and σ_f is the standard deviation characterizing the statistical uncertainty in f . Instead of relying on asymptotic properties of the likelihood (Wilks' theorem S. S. Wilks 1938), we compute σ_f empirically by repeating the analysis on many simulated datasets with the same configuration. This Monte Carlo procedure provides a more robust estimate of the confidence interval for f , particularly in regimes where the number of signal events is small.

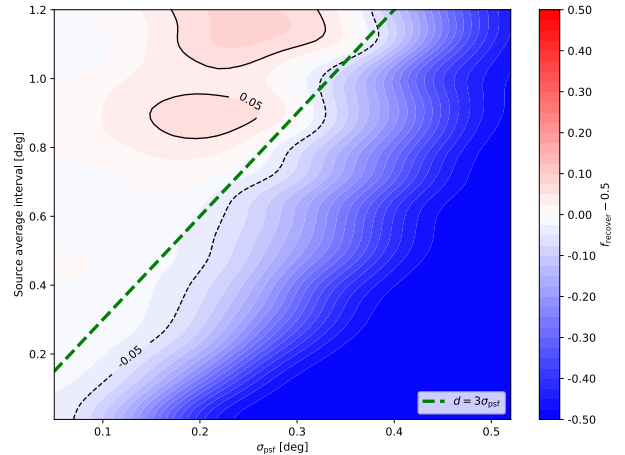


Figure 1. Deviation of the recovered signal fraction from the true value, $f_{\text{recover}} - 0.5$, as a function of PSF and average source separation. Red (blue) regions indicate positive (negative) deviations, while the white region corresponds to no bias (i.e., $f_{\text{recover}} = 0.5$). The green dashed line marks $d = 3\sigma_{\text{psf}}$, above which the recovered fraction converges to the true value $f_{\text{recover}} = 0.5$.

3.2. Mitigating Source Confusion in ML

Likelihood-based methods provide a powerful statistical framework for estimating the neutrino signal fraction f . However, it does not sufficiently address the impact of source confusion—a fundamental limitation in astronomical surveys that arises when the instrument’s angular resolution is too coarse to distinguish nearby sources (X. Barcons 1992). As also noted by M. Kowalski et al. (2025), stacking becomes unreliable when the average number of sources within a single PSF exceeds one, resulting in systematic underestimate of f .

To quantify this effect, we investigate how the mean angular separation between sources (\bar{d}) interacts with the detector’s PSF width (σ_{psf}). Since brighter sources tend to be more sparsely distributed, adjusting F_{min} provides a practical way to control the source density. Specifically, we define a minimum separation d and determine the corresponding F_{min} such that the selected AGNs have a typical spacing larger than \bar{d} . This approach allows us to explore a wide range of source densities while maintaining physical realism.

Figure 1 summarizes the results for a fixed true value $f = 0.5$. When the average separation satisfies $\bar{d} \gtrsim 3\sigma_{\text{psf}}$, the maximum-likelihood estimator reliably recovers the true f . In contrast, for denser source populations ($\bar{d} \lesssim 3\sigma_{\text{psf}}$), confusion effects cause f to be systematically underestimated. This yields a practical condition for method applicability: the source population must be sufficiently sparse, such that the average spacing between sources exceeds approximately three times

the PSF width. Importantly, we verify that this trend is valid for a wide range of values of f , not just for the specific case of $f = 0.5$.

Based on this empirical criterion, we set a threshold of X-ray flux F_{\min} for AGNs chosen in all subsequent analyses, so that chosen subset of AGNs with $F_X \geq F_{\min}$ satisfy $d > 3\sigma_{\text{psf}}$. This ensures that the selected AGN population remains well-resolved, thereby mitigating confusion-induced bias and preserving the validity of the maximum-likelihood inference. The chosen subset therefore represents only the relatively bright portion of the whole AGN population. To infer the total neutrino contribution from the whole AGN population, we compute a correction factor based on the cumulative flux ratio between the flux-limited subset and the full sample:

$$f_{\text{total}} = f_{\text{bright}} \cdot \frac{\sum_{\text{all}} F_X}{\sum_{F_X > F_{\min}} F_X}, \quad (5)$$

where f_{bright} is the fraction inferred from the likelihood analysis of the bright subset. This scaling accounts for the contribution of unresolved faint sources that are excluded by the F_{\min} cut. All reported values of f in this work, including those shown in Figure 1, incorporate this flux-based correction to ensure consistency with the full AGN population, even though the likelihood analysis itself is restricted to the bright, confusion-free subset.

4. PREDICTIVE POWER FOR FUTURE NEUTRINO DETECTORS

Next-generation neutrino observatories are expected to greatly enhance the capability to detect astrophysical neutrino sources. Proposed facilities such as IceCube-Gen2, HUNT, TRIDENT, NEON and Baikal-GVD, also promise enhanced exposure and angular resolution. These advancements motivate us to examine how the improvements in angular resolution, event statistics, and energy threshold affect the prospects for diagnosing the neutrino–AGN correlation.

We perform a series of simulations to quantify how key observational parameters influence the detection potential. Specifically, we examine four primary factors: the detector’s angular resolution, the total number of detected neutrinos, the minimum energy threshold, and the observation duration. These variables determine both the statistical power and the level of background contamination, which jointly govern the overall sensitivity of correlation searches.

Figure 2 illustrates how the detection significance depends jointly on the angular resolution and the total number of detected neutrinos, using **a sample of events** with reconstructed energies above 100 TeV,

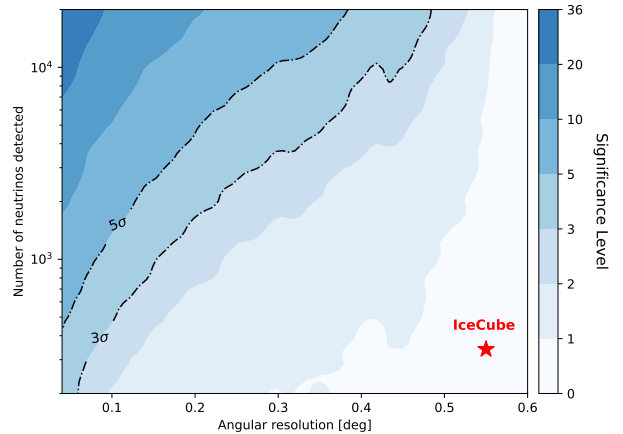


Figure 2. Detection significance as a function of angular resolution and the total number of detected neutrinos. The color map indicates the significance level, with solid and dashed contours marking the 5σ and 3σ confidence levels, respectively. The gold star denotes the parameter point corresponding to the *IceCube Alert* event (A. Zegarelli et al. 2025).

where the astrophysical neutrino fraction is fixed at $f = 0.5$. The trends are clear: improving the angular resolution reduces positional uncertainties, thereby increasing the contrast between AGN–neutrino associations and random coincidences. At a fixed angular resolution, increasing the total event count enhances the statistical weight of the likelihood, roughly following the expected $(S/N)_f \propto \sqrt{N}$ scaling. Conversely, when the number of detected neutrinos is fixed, the significance scales approximately with the inverse of the PSF width, i.e. $(S/N)_f \propto \sigma_{\text{psf}}^{-1}$. Notably, achieving a 5σ detection requires only ~ 2000 events when the angular resolution is as fine as 0.1° , whereas resolution coarser than 0.4° demands orders of magnitude more events, making such significance practically unattainable. At present, IceCube’s effective exposure and angular resolution limit the attainable significance: with $\sim 10^2$ – 10^3 detected astrophysical neutrinos and a median angular uncertainty of $\sim 0.55^\circ$ for above 100 TeV (A. Zegarelli et al. 2025), the current data fall short of the regime where AGN population correlations could be statistically established (denoted by “IceCube” in Figure 2). This highlights angular resolution as the dominant driver of sensitivity. This trend can be explained as arising from two effects: (i) a narrower σ_{psf} allows inclusion of a larger portion of the AGN population—including contributions from fainter sources that would otherwise be lost in confusion noise; and (ii) improved localization concentrates the signal probability density closer to the true source positions, thereby increasing the likelihood ratio and boosting the test statistic.

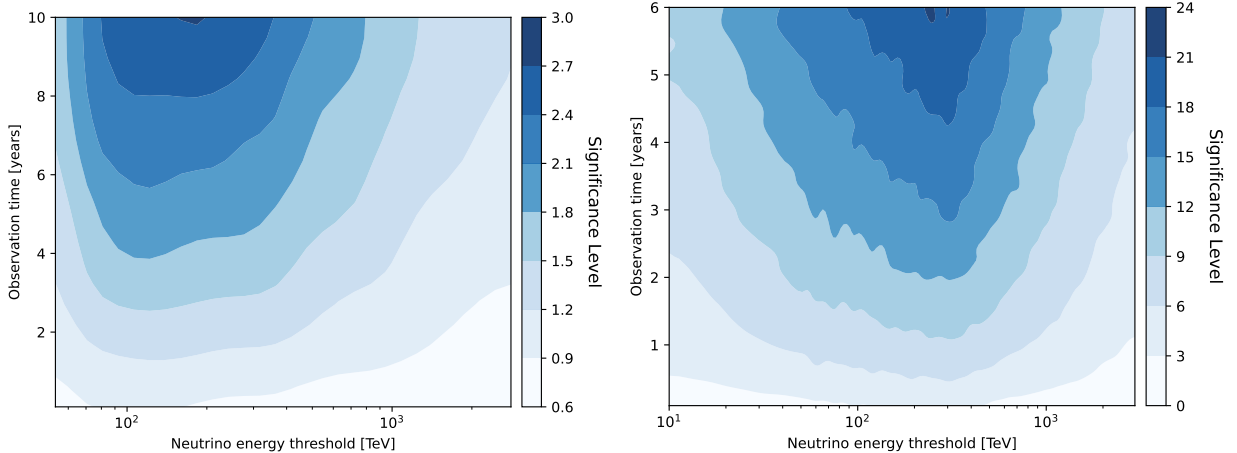


Figure 3. Trade-off between neutrino energy threshold and exposure time for future neutrino observatories. **The left panel** shows results for IceCube-Gen2, adopting the projected energy-dependent angular resolution from [E. Blaufuss et al. \(2019\)](#). **The right panel** shows the corresponding results for the proposed 30 km³ HUNT detector, incorporating its energy-dependent angular resolution and effective area (private communication with Tian-Qi Huang).

Building upon the angular resolution-based considerations described above, we next examine how the selection of different neutrino energy bands influences the source identification capabilities. In particular, the fraction of detected neutrino events above a given energy threshold plays a key role in the achievable signal-to-noise ratio: astrophysical neutrinos from AGN are expected to dominate at higher energies, while the atmospheric background falls steeply. Moreover, higher-energy neutrinos are reconstructed with better angular resolution, further enhancing source identification capabilities.

Figure 3 illustrates the trade-off between neutrino energy threshold and exposure time for future neutrino observatories, with the left panel corresponding to IceCube-Gen2 and the right panel to the proposed HUNT detector. The horizontal axis denotes the minimum reconstructed neutrino energy threshold applied to the event sample, while the vertical axis indicates the observation time required to reach a given detection significance. For IceCube-Gen2, the energy-dependent angular resolution is adopted from the projected point-spread function reported in [E. Blaufuss et al. \(2019\)](#), while for the HUNT detector the calculation incorporates its energy-dependent angular resolution and effective area (private communication with Tian-Qi Huang).

As the energy threshold of neutrinos increases, two competing effects emerge: (i) the angular resolution improves and the atmospheric neutrino flux drops; (ii) the number of neutrino events above the energy threshold declines, reducing statistical power. These opposing trends jointly define an optimal energy window, typically around a few hundred TeV, where the sensitivity peaks. Beyond this point, further increases in the en-

ergy threshold yield diminishing returns due to low event rates. Owing to the expected angular resolution of the HUNT detector being improved by a factor of ~ 4 – 5 relative to IceCube-Gen2, together with an effective area larger by a factor of ~ 3 , the HUNT detector naturally achieves a higher detection significance for a given energy threshold and exposure time.

5. IMPACT OF SYSTEMATIC AND POSITIONAL UNCERTAINTIES

The analyses presented thus far assumed idealized conditions: the AGN X-ray luminosity function (XLF) was treated as perfectly known, and the neutrino angular uncertainty was assumed to be fixed for all events. In practice, both assumptions introduce additional uncertainties in the inferred signal fraction f . Here we quantify the contributions from these two dominant sources of uncertainty and evaluate their combined impact on the overall detection significance.

The first source of uncertainty arises from the extrapolation of the bright AGN subsample (above F_{\min}) to the entire AGN population. In our baseline approach, this extrapolation is carried out using the luminosity distribution of the eFEDS AGN catalog, which provides direct observational data and avoids the need for an explicit parametric model. However, the eFEDS sample does not fully capture the global AGN population, particularly at low luminosities and high redshifts. To assess this systematic, we perform an alternative extrapolation based on the parametric AGN XLF. Assuming a linear relation between neutrino and X-ray luminosities (e.g., [R. Abbasi et al. 2022](#); [E. Kun et al. 2024](#)), the

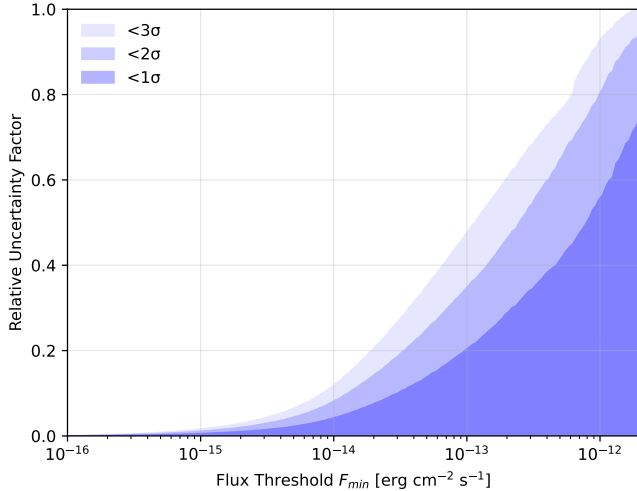


Figure 4. Relative uncertainty factor in the extrapolated AGN contribution as a function of the flux threshold F_{\min} . The blue line shows the mean correction factor, and shaded regions indicate 1σ , 2σ , and 3σ confidence intervals. Uncertainties remain modest at low thresholds but grow rapidly when only the brightest AGNs are included.

total neutrino flux is expressed as

$$\Phi_{\nu}^{\text{tot}} \propto \int_{L_{\min}}^{L_{\max}} L_X \phi(L_X, z) dL_X dz, \quad (6)$$

where $\phi(L_X, z)$ is the XLF. Using the best-fit parameters and reported uncertainties from recent XLF measurements (Y. Ueda et al. 2014), we propagate parameter variations through Monte Carlo simulations to estimate the relative uncertainty in the extrapolated neutrino contribution as a function of the X-ray flux threshold F_{\min} . The resulting uncertainty is summarized in Figure 4. As expected, adopting brighter flux thresholds leads to significantly larger uncertainties. This arises because selecting only the most luminous AGNs (e.g., $F_{\min} > 3 \times 10^{-13} \text{ erg cm}^{-2} \text{ s}^{-1}$) leaves the majority of the AGN population unresolved; extrapolation from such a small subset amplifies the impact of uncertainties in the faint-end slope and normalization of the XLF, potentially causing the correction factor to vary by factors of several. In these extreme cases, the extrapolation becomes unreliable and the inferred total neutrino contribution cannot be robustly constrained. Therefore, this method is only recommended for flux thresholds below $\sim 2 \times 10^{-13} \text{ erg cm}^{-2} \text{ s}^{-1}$, where the extrapolation remains well-behaved.

The second source of uncertainty stems from event-by-event variations in the σ_{psf} . In previous sections, we adopted a fixed PSF width σ_{psf} for a given energy bin, whereas real detectors exhibit a distribution of reconstructed angular uncertainties. This variation effec-

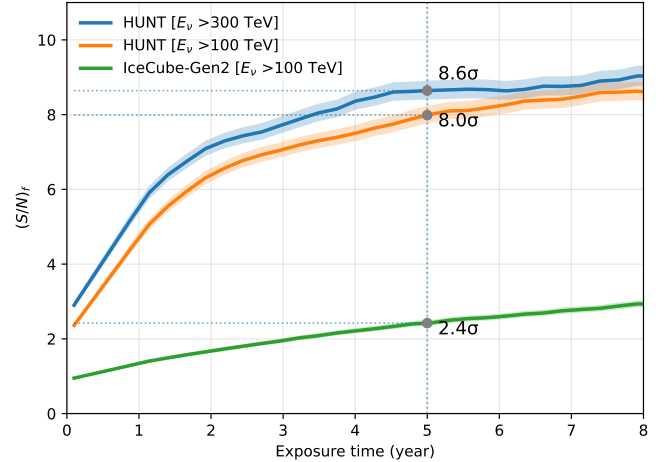


Figure 5. Expected Detection significance as a function of exposure time for different detector configurations and energy selections. The vertical dotted line indicates an exposure of 5 yr, with the corresponding $(S/N)_f$ values marked for comparison.

tively broadens the signal and background probability density functions used in the maximum-likelihood analysis, thereby reducing sensitivity. To quantify this effect, we simulate neutrino samples by assigning to each event a σ_{psf} randomly sampled from the detector’s energy-dependent angular resolution distribution.

Combining the uncertainties from both XLF extrapolation and PSF variation, we assess the sensitivity of future neutrino telescopes to testing the AGN-origin hypothesis. As a more generic and near-term scenario, we first consider a 10 km^3 undersea neutrino telescope with an angular resolution of 0.2° , representative of IceCube-Gen2. We include all neutrino events with energies above 100 TeV and select the full AGN sample with X-ray fluxes $F_X > 2.4 \times 10^{-13} \text{ erg s}^{-1} \text{ cm}^{-2}$. The uncertainty associated with the extrapolation of the XLF is modeled as a relative error of 30%. Under these assumptions, such a detector would achieve a significance of approximately 2.4σ after five years of exposure in testing whether all astrophysical neutrinos originate from AGNs, as shown in the Figure 5. This level of significance, while suggestive, is insufficient for a decisive test of the AGN-origin hypothesis.

As an illustrative and more optimistic case, we consider a 30 km^3 neutrino detector and focus on events with energies above 300 TeV, where an angular resolution of 0.04° is expected. At this energy threshold, we restrict the analysis to AGNs with X-ray fluxes $F_X > 4 \times 10^{-14} \text{ erg s}^{-1} \text{ cm}^{-2}$. The uncertainty arising from the extrapolation of the X-ray luminosity function is again treated as a relative error of 10%, and variations in the detector PSF are also taken into account.

Under this configuration, a 30km^3 detector can test the AGN-origin hypothesis at a confidence level of roughly 8.6σ after three years of exposure, even after accounting for both XLF extrapolation and σ_{psf} variation uncertainties, as shown in the Figure 5. We further explore a broader energy range of above 100 TeV. In this case, the expected significance is 8σ after five years of exposure. The limited improvement despite increased statistics highlights the dominant role of XLF extrapolation uncertainties, which ultimately constrain further sensitivity gains.

6. DISCUSSION

6.1. AGN as a Fractional Source of the Diffuse neutrino Flux

Throughout most of this work we have illustrated the methodology using the limiting case in which AGNs are assumed to be the dominant contributors to the observed astrophysical neutrino flux. In reality, the diffuse neutrino background could be produced by a mixture of source populations, and AGNs may account for only a fraction of the total. Our framework readily accommodates this more general scenario: the parameter f in the unbinned maximum-likelihood formalism already represents the fraction of events associated with AGNs, while the remaining $(1 - f)$ fraction is treated as isotropic background.

Figure 6 (left) demonstrates how the signal-to-noise ratio $(S/N)_f$ scales with f for a representative next-generation detector scenario (a 30km^3 -scale underwater neutrino telescope with 3 years of exposure). The trend is nearly linear, indicating that even modest AGN contributions (e.g., $f \sim 0.2$) remain detectable at $\sim 4\sigma$ significance. This scaling behavior arises because the likelihood ratio effectively isolates the spatially correlated AGN component, which diminishes proportionally with f , while the statistical background remains unchanged.

6.2. X-ray flux-weighting

Our main assumption is a linear relationship between the number of neutrinos and the AGN X-ray flux. Even if this linearity holds, different AGN classes may exhibit distinct proportionality constants due to underlying physical differences (I. B. Jacobsen et al. 2015; A. Ambrosone 2024). To generalize this idea, we explore a family of models in which the neutrino yield from each AGN scales with its X-ray flux as $N_\nu \propto F_X^s$. The parameter s reflects the assumed physical correlation strength: $s = 0$ corresponds to no dependence (i.e., uniform weighting across AGNs), while increasing s emphasizes the role of brighter AGNs in neutrino production. In this case, the source weights in Equation 2 of

the likelihood function are modified to $w_\alpha = F_\alpha^s / \sum_k F_k^s$ ensuring that the simulated neutrino–AGN associations reflect the chosen correlation index s .

Figure 6 (right) demonstrates the signal-to-noise ratio $(S/N)_f$ as a function of s using a 30km^3 neutrino telescope over three years of exposure. The results indicate a monotonic increase in $(S/N)_f$ with s , reflecting the growing dominance of bright AGNs in neutrino production. For $s \approx 0$, corresponding to uniform weighting, the detection significance is limited to $\sim 3\sigma$. As s increases toward unity—implying a direct proportionality between neutrino and X-ray flux—the significance improves substantially. This trend suggests that if neutrino emission preferentially traces the most luminous AGNs, the detectability of the population-level correlation is considerably enhanced. Conversely, a flatter weighting ($s < 0.5$) implies that fainter AGNs contribute more evenly, reducing the overall signal contrast relative to the isotropic background.

6.3. Blazars Neutrino Predictions

Blazars are also thought to be possible sources of extragalactic neutrinos, and are likely to contribute a significant fraction in the diffuse neutrino intensity at sub-PeV energies (e.g., K. Murase et al. 2014; IceCube Collaboration et al. 2018; S. Buson et al. 2022). Motivated by the association of TXS 0506+056 with a hard-spectrum ($\Gamma \approx 2$) neutrino flare, we focus on the contribution of blazars to neutrinos above ~ 100 TeV, where such sources are expected to be more prominent.

To directly test this scenario, IceCube has performed dedicated searches for cumulative emission from GeV-selected blazar populations (M. G. Aartsen et al. 2017). No significant excess was observed, and the upper limits constrain the contribution of 2LAC blazars to $\lesssim 27\%$ of the observed diffuse neutrino flux between 10 TeV and 2 PeV (for a spectral index $\Gamma = 2.5$). Nevertheless, it is reasonable to expect that their relative contribution becomes more significant above ~ 100 TeV, motivating us to focus on this higher-energy regime in assessing the role of blazars as neutrino sources.

We consider the 3933 classified as blazars from the fourth Fermi-LAT catalog (J. Ballet et al. 2023), which includes 820 flat spectrum radio quasars (FSRQs), 1490 BL Lacs, and 1623 other sources classified as "blazars of unknown type". We extrapolate their collective neutrino contribution using the GeV gamma-ray luminosity function (GLF) (S. Manconi et al. 2020), following the same procedure as that applied to the AGN X-ray luminosity function (XLF) in Section 5. Figure 7 (left) presents the cumulative fraction of the total blazar neutrino flux as a function of flux threshold, with shaded re-

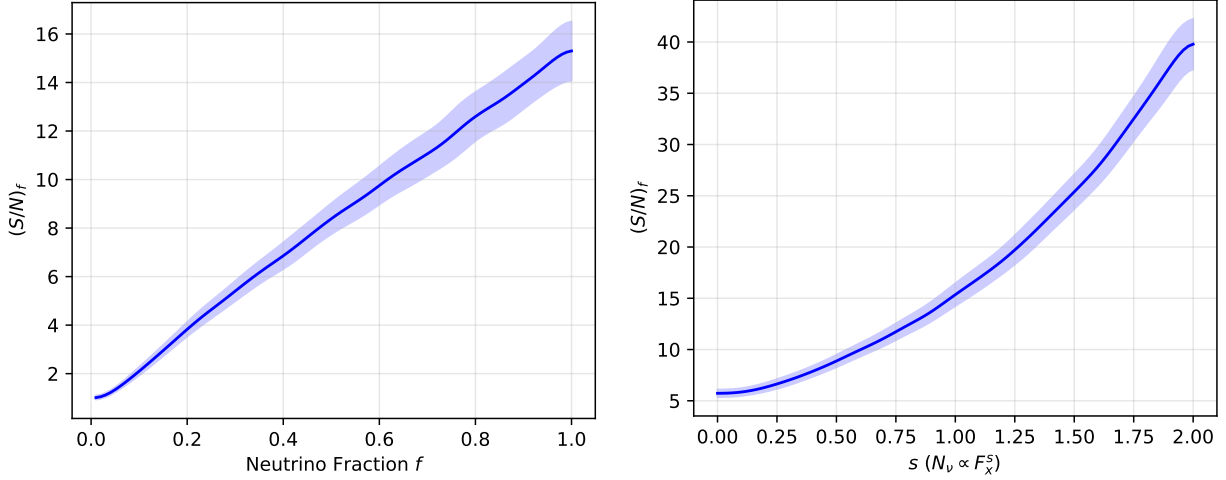


Figure 6. **Left:** Signal-to-noise ratio $(S/N)_f$ as a function of neutrino fraction f , showing that even partial AGN contributions can be constrained with high significance. **Right:** $(S/N)_f$ as a function of the flux-weighting parameter s ($N_\nu \propto F_X^s$), illustrating that stronger weighting toward luminous AGNs enhances detectability. All panels correspond to a 30 km^3 undersea neutrino telescope with 3 years of exposure.

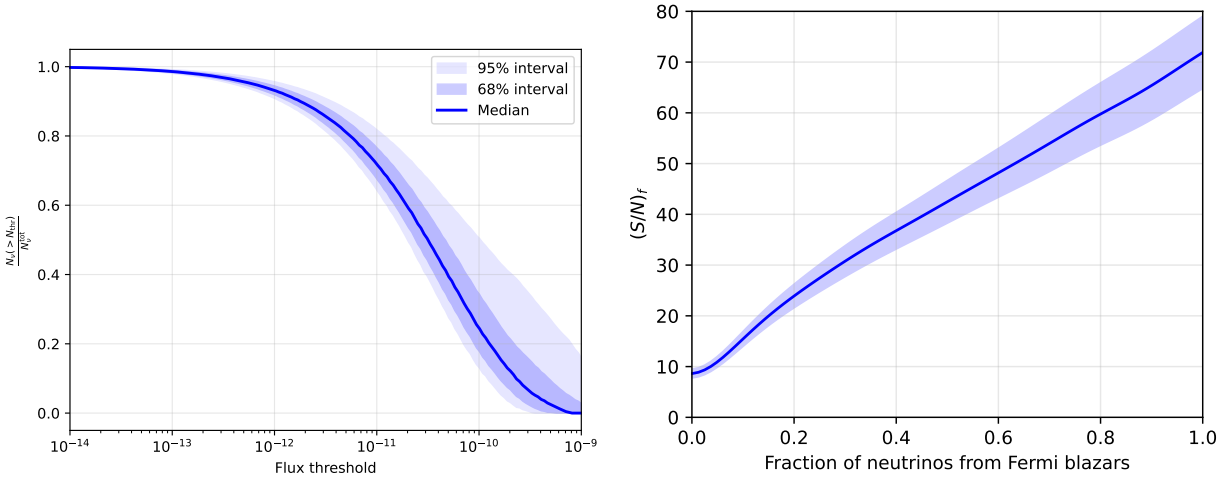


Figure 7. **Left:** Cumulative fraction of the total neutrinos contributed by blazars with flux above a given threshold. The solid line shows the median, while the shaded regions indicate the 68% and 95 % credible intervals. **Right:** $(S/N)_f$ for the cumulative blazars contribution above 100 TeV, evaluated as a function of the assumed blazars fraction of the diffuse neutrino flux with a 30 km^3 undersea neutrino telescope with 3 years of exposure.

gions showing the 68% and 95% credible intervals. Here, the “flux threshold” corresponds to the average energy flux detection limit of Fermi-LAT, representing the approximate completeness threshold of the blazar sample. Given that the mean sensitivity limit for the Fermi-LAT blazar sample is about $2 \times 10^{-12} \text{ erg s}^{-1} \text{ cm}^{-2}$ (M. Ajello et al. 2022), we estimate that this Fermi-LAT blazar population accounts for approximately $\sim 85\% \pm 5\%$ of the total neutrino emission from all blazars. Figure 7 (right) illustrates the trend of the detection significance as a function of the assumed blazars fraction for a 30 km^3 detector over 3 years.

When systematic effects are included, the dominant limitation arises from GLF uncertainties. In this case, if blazars contribute to $\sim 5\%$ of the diffuse neutrino flux above 100 TeV, our method reaches a 5σ detection significance for 3 years of exposure. For larger assumed fractions, the significance does not further increase, since the GLF uncertainties impose a systematic floor on the achievable sensitivity. This demonstrates that our approach is capable of identifying even a modest blazar contribution to the diffuse neutrino flux with high confidence. In particular, the ability to reach a 5σ signifi-

cance level for a $\sim 5\%$ contribution highlights the strong discovery potential of the method.

6.4. Implications of a Two-Population AGN Scenario

The current evidence suggests that different classes of AGNs may contribute neutrinos in distinct energy bands. The case of NGC 1068 (IceCube Collaboration et al. 2022) indicates that at least some Seyfert galaxies predominantly produce neutrinos at relatively low energies ($E_\nu < 100$ TeV). In contrast, the presence of > 100 TeV neutrinos in the direction of NGC 7469 (although not yet statistically significant, G. Sommani et al. 2025) or TXS 0506+056 (IceCube Collaboration et al. 2018) hints at the possibility that another subclass of AGNs could be responsible for the high-energy tail of the diffuse neutrino spectrum (Yang et al. in preparation). These considerations motivate a two-population AGN scenario, in which (i) NGC 1068-like sources dominate the low-energy neutrino flux, while (ii) a different population, potentially blazar-like or luminous Seyferts with favorable conditions for hard neutrino spectrum, contributes primarily to the > 100 TeV neutrino flux. The diffuse astrophysical neutrino background would then emerge as a superposition of these two populations.

We further examined the simplified hypothesis that neutrinos with $E_\nu > 100$ TeV are predominantly produced by a subset of the AGN population ('hard' AGN). Since the physical origin of such hard-spectrum AGNs is not yet identified, we randomly select a given fraction (e.g., 25% or 50%) of the AGN sample to represent this subpopulation in our simulations. Compared to the assumption that the entire AGN population contributes to the diffuse flux, restricting the contribution to only a fraction of AGNs effectively increases the weight assigned to each source in the likelihood analysis. Such hard-spectrum AGNs may feature higher proton acceleration efficiencies or denser photon fields, enhancing $p\gamma$ interactions at higher energies. This reduced source population strengthens the contrast between signal and background, thereby enhancing the achievable confidence level of detection. In the future, more refined AGN neutrino models may allow us to classify sources based on physical parameters that naturally lead to either soft or hard neutrino spectra. Such developments would provide a critical pathway to test whether a small subset of hard AGNs indeed dominates the diffuse neutrino flux above 100 TeV.

At the same time, it should be noted that the dominant source of systematic uncertainty remains in the X-ray luminosity function of AGNs, as discussed in Sec. 5. This implies that the ultimate confidence level for testing the hard-AGN hypothesis is limited by the same

luminosity-function uncertainties as in the baseline analysis. Nevertheless, the method remains robust and provides a promising avenue to probe whether a fraction of AGNs with harder spectra are the main contributors to the diffuse neutrino flux above 100 TeV.

7. CONCLUSION

We have presented a comprehensive framework to evaluate the detectability of correlations between high-energy neutrinos and AGNs, incorporating both statistical and systematic effects. Our analysis combines flux-weighted likelihood methods with realistic detector performance and observational constraints. The key findings are summarized as follows:

- **Dominant role of angular resolution:** The sensitivity of AGN–neutrino correlation searches is primarily driven by the detector’s point-spread function. Achieving sub-degree resolution, particularly $\lesssim 0.1^\circ$, dramatically reduces background contamination and enhances detection significance. For example, with 2000 events and a 0.1° resolution, a 5σ detection is achievable, whereas resolutions coarser than 0.4° would require orders of magnitude more events.
- **Source separation criterion:** To minimize source confusion and ensure robust association between neutrinos and AGNs, we require the mean angular separation between selected AGNs to exceed three times the detector’s PSF width ($\bar{d} > 3\sigma_{\text{psf}}$). This criterion effectively avoids source confusion, yielding a cleaner AGN sample for correlation analysis and more reliable flux extrapolations to the full population.
- **Energy threshold optimization:** Increasing the minimum neutrino energy threshold improves angular resolution and suppresses atmospheric backgrounds, but reduces event statistics. For a 30 km^3 undersea neutrino telescope (e.g., HUNT) that features rapidly improving resolution with energy (down to $\sim 0.04^\circ$ above 300 TeV), the optimal sensitivity is reached at thresholds of a few hundred TeV. In contrast, IceCube-Gen2 shows weaker energy dependence in its resolution; for this detector, selecting $E_\nu > 100$ TeV strikes a better balance between angular precision and event statistics.
- **Flux-limited AGN extrapolation and XLF systematics:** Our likelihood analysis is performed on a flux-limited AGN subset ($\bar{d} > 3\sigma_{\text{psf}}$), and the total neutrino contribution is inferred via

extrapolation to the full AGN population. The extrapolation uncertainty is dominated by the flux threshold F_{\min} : for $F_{\min} \lesssim 10^{-14}$ erg cm $^{-2}$ s $^{-1}$ the uncertainty is small ($\lesssim 10\%$), while $F_{\min} \gtrsim 3 \times 10^{-13}$ erg cm $^{-2}$ s $^{-1}$ yields unreliable results due to the dominance of faint AGNs in the XLF. In addition, accounting for realistic distributions of reconstructed event angles introduces an additional $\sim 10\%$ uncertainty in the inferred AGN neutrino fraction f , particularly affecting low-energy dominated samples. This highlights the importance of incorporating per-event angular information in future analyses.

- **Implications for next-generation neutrino telescopes:** In the above 1300 TeV energy range, a 30 km 3 undersea neutrino telescope is expected to reach a significance of 8.6σ after five years of

exposure. The limited improvement despite the larger statistics reflects the dominant impact of XLF extrapolation uncertainties, which ultimately set a systematic floor on the achievable sensitivity. For IceCube-Gen2, with $\sim 0.2^\circ$ resolution above 100 TeV, the achievable confidence level is $\sim 2.4\sigma$ over five years.

These results demonstrate that next-generation neutrino observatories with sub-degree angular precision and sufficient exposure have the potential to either confirm or strongly constrain the AGN origin of high-energy neutrinos. Deep multi-wavelength AGN surveys, especially in X-rays, are crucial to minimize uncertainties in flux extrapolation and to fully exploit the discovery potential of upcoming facilities.

We thank Tian-Qi Huang and Siqi Yu for valuable discussions.

REFERENCES

- Aartsen, M. G., Abraham, K., Ackermann, M., et al. 2017, The Contribution of Fermi-2LAC Blazars to Diffuse TeV-PeV Neutrino Flux, *ApJ*, 835, 45, doi: [10.3847/1538-4357/835/1/45](https://doi.org/10.3847/1538-4357/835/1/45)
- Aartsen, M. G., Ackermann, M., Adams, J., et al. 2020a, Time-Integrated Neutrino Source Searches with 10 Years of IceCube Data, *PhRvL*, 124, 051103, doi: [10.1103/PhysRevLett.124.051103](https://doi.org/10.1103/PhysRevLett.124.051103)
- Aartsen, M. G., Ackermann, M., Adams, J., et al. 2020b, Characteristics of the Diffuse Astrophysical Electron and Tau Neutrino Flux with Six Years of IceCube High Energy Cascade Data, *PhRvL*, 125, 121104, doi: [10.1103/PhysRevLett.125.121104](https://doi.org/10.1103/PhysRevLett.125.121104)
- Aartsen, M. G., Abbasi, R., Ackermann, M., et al. 2021, IceCube-Gen2: the window to the extreme Universe, *Journal of Physics G Nuclear Physics*, 48, 060501, doi: [10.1088/1361-6471/abbd48](https://doi.org/10.1088/1361-6471/abbd48)
- Abbasi, R., Ackermann, M., Adams, J., et al. 2022, Improved Characterization of the Astrophysical Muon-Neutrino Flux with 9.5 Years of IceCube Data, *The Astrophysical Journal*, 928, 50, doi: [10.3847/1538-4357/ac4d29](https://doi.org/10.3847/1538-4357/ac4d29)
- Abbasi, R., Ackermann, M., Adams, J., et al. 2022, Search for neutrino emission from cores of active galactic nuclei, *PhRvD*, 106, 022005, doi: [10.1103/PhysRevD.106.022005](https://doi.org/10.1103/PhysRevD.106.022005)
- Abbasi, R., Ackermann, M., Adams, J., et al. 2023, Search for Correlations of High-energy Neutrinos Detected in IceCube with Radio-bright AGN and Gamma-Ray Emission from Blazars, *ApJ*, 954, 75, doi: [10.3847/1538-4357/acdfcb](https://doi.org/10.3847/1538-4357/acdfcb)
- Abbasi, R., Ackermann, M., Adams, J., et al. 2024, Probing the Connection between IceCube Neutrinos and MOJAVE AGN, *ApJ*, 973, 97, doi: [10.3847/1538-4357/ad643d](https://doi.org/10.3847/1538-4357/ad643d)
- Abbasi, R., Ackermann, M., Adams, J., et al. 2025a, Evidence for Neutrino Emission from X-ray Bright Active Galactic Nuclei with IceCube, arXiv e-prints, arXiv:2510.13403, doi: [10.48550/arXiv.2510.13403](https://doi.org/10.48550/arXiv.2510.13403)
- Abbasi, R., Ackermann, M., Adams, J., et al. 2025b, Search for Neutrino Emission from Hard X-Ray AGN with IceCube, *ApJ*, 981, 131, doi: [10.3847/1538-4357/ada94b](https://doi.org/10.3847/1538-4357/ada94b)
- Acciari, V. A., Ansoldi, S., Antonelli, L. A., et al. 2019, Constraints on Gamma-Ray and Neutrino Emission from NGC 1068 with the MAGIC Telescopes, *ApJ*, 883, 135, doi: [10.3847/1538-4357/ab3a51](https://doi.org/10.3847/1538-4357/ab3a51)
- Ackermann, M., Ajello, M., Albert, A., et al. 2015, The Spectrum of Isotropic Diffuse Gamma-Ray Emission between 100 MeV and 820 GeV, *ApJ*, 799, 86, doi: [10.1088/0004-637X/799/1/86](https://doi.org/10.1088/0004-637X/799/1/86)
- Adrián-Martínez, S., Ageron, M., Aharonian, F., et al. 2016, Letter of intent for KM3NeT 2.0, *Journal of Physics G Nuclear Physics*, 43, 084001, doi: [10.1088/0954-3899/43/8/084001](https://doi.org/10.1088/0954-3899/43/8/084001)

- Ajello, M., Baldini, L., Ballet, J., et al. 2022, The Fourth Catalog of Active Galactic Nuclei Detected by the Fermi Large Area Telescope: Data Release 3, *ApJS*, 263, 24, doi: [10.3847/1538-4365/ac9523](https://doi.org/10.3847/1538-4365/ac9523)
- Ambrosone, A. 2024, Berezinsky Hidden Sources: An Emergent Tension in the High-Energy Neutrino Sky? arXiv, doi: [10.48550/ARXIV.2406.13336](https://doi.org/10.48550/ARXIV.2406.13336)
- Ballet, J., Bruel, P., Burnett, T. H., Lott, B., & The Fermi-LAT collaboration. 2023, Fermi Large Area Telescope Fourth Source Catalog Data Release 4 (4FGL-DR4), arXiv e-prints, arXiv:2307.12546, doi: [10.48550/arXiv.2307.12546](https://doi.org/10.48550/arXiv.2307.12546)
- Barcons, X. 1992, Confusion Noise and Source Clustering, *ApJ*, 396, 460, doi: [10.1086/171733](https://doi.org/10.1086/171733)
- Bechtol, K., Ahlers, M., Di Mauro, M., Ajello, M., & Vandenbroucke, J. 2017, Evidence against Star-forming Galaxies as the Dominant Source of Icecube Neutrinos, *ApJ*, 836, 47, doi: [10.3847/1538-4357/836/1/47](https://doi.org/10.3847/1538-4357/836/1/47)
- Belolaptikov, I., Dzhilkibaev, Z. A. M., Allakhverdyan, V. A., et al. 2022, in 37th International Cosmic Ray Conference, 2, doi: [10.22323/1.395.002](https://doi.org/10.22323/1.395.002)
- Blaufuss, E., Kintscher, T., Lu, L., & Tung, C. F. 2019, in International Cosmic Ray Conference, Vol. 36, 36th International Cosmic Ray Conference (ICRC2019), 1021, doi: [10.22323/1.358.01021](https://doi.org/10.22323/1.358.01021)
- Braun, J., Dumm, J., De Palma, F., et al. 2008, Methods for Point Source Analysis in High Energy Neutrino Telescopes, *Astroparticle Physics*, 29, 299, doi: [10.1016/j.astropartphys.2008.02.007](https://doi.org/10.1016/j.astropartphys.2008.02.007)
- Buson, S., Tramacere, A., Pfeiffer, L., et al. 2022, Beginning a Journey Across the Universe: The Discovery of Extragalactic Neutrino Factories, *ApJL*, 933, L43, doi: [10.3847/2041-8213/ac7d5b](https://doi.org/10.3847/2041-8213/ac7d5b)
- Capanema, A., Esmaili, A., & Murase, K. 2020, New constraints on the origin of medium-energy neutrinos observed by IceCube, *PhRvD*, 101, 103012, doi: [10.1103/PhysRevD.101.103012](https://doi.org/10.1103/PhysRevD.101.103012)
- Creque-Sarbinowski, C., Kamionkowski, M., & Zhou, B. 2022, Seeking Neutrino Emission from AGN through Temporal and Spatial Cross-Correlation, *Physical Review D*, 105, 123035, doi: [10.1103/PhysRevD.105.123035](https://doi.org/10.1103/PhysRevD.105.123035)
- Eichmann, B., Oikonomou, F., Salvatore, S., Dettmar, R.-J., & Tjus, J. B. 2022, Solving the Multimessenger Puzzle of the AGN-starburst Composite Galaxy NGC 1068, *ApJ*, 939, 43, doi: [10.3847/1538-4357/ac9588](https://doi.org/10.3847/1538-4357/ac9588)
- Fang, K., Gallagher, J. S., & Halzen, F. 2022, The TeV Diffuse Cosmic Neutrino Spectrum and the Nature of Astrophysical Neutrino Sources, *ApJ*, 933, 190, doi: [10.3847/1538-4357/ac7649](https://doi.org/10.3847/1538-4357/ac7649)
- Fiorillo, D. F. G., Comisso, L., Peretti, E., Petropoulou, M., & Sironi, L. 2025, The contribution of turbulent AGN coronae to the diffuse neutrino flux, arXiv e-prints, arXiv:2504.06336, doi: [10.48550/arXiv.2504.06336](https://doi.org/10.48550/arXiv.2504.06336)
- Huang, T. Q., Cao, Z., Chen, M., et al. 2024, in 38th International Cosmic Ray Conference, 1080
- IceCube Collaboration, Aartsen, M. G., Ackermann, M., et al. 2018, Neutrino emission from the direction of the blazar TXS 0506+056 prior to the IceCube-170922A alert, *Science*, 361, 147, doi: [10.1126/science.aat2890](https://doi.org/10.1126/science.aat2890)
- IceCube Collaboration, Abbasi, R., Ackermann, M., et al. 2022, Evidence for neutrino emission from the nearby active galaxy NGC 1068, *Science*, 378, 538, doi: [10.1126/science.abg3395](https://doi.org/10.1126/science.abg3395)
- Inoue, Y., Khangulyan, D., & Doi, A. 2020, On the Origin of High-energy Neutrinos from NGC 1068: The Role of Nonthermal Coronal Activity, *ApJL*, 891, L33, doi: [10.3847/2041-8213/ab7661](https://doi.org/10.3847/2041-8213/ab7661)
- Jacobsen, I. B., Wu, K., On, A. Y. L., & Saxton, C. J. 2015, High-Energy Neutrino Fluxes from AGN Populations Inferred from X-ray Surveys, *Monthly Notices of the Royal Astronomical Society*, 451, 3649, doi: [10.1093/mnras/stv1196](https://doi.org/10.1093/mnras/stv1196)
- Kheirandish, A., Murase, K., & Kimura, S. S. 2021, High-energy Neutrinos from Magnetized Coronae of Active Galactic Nuclei and Prospects for Identification of Seyfert Galaxies and Quasars in Neutrino Telescopes, *ApJ*, 922, 45, doi: [10.3847/1538-4357/ac1c77](https://doi.org/10.3847/1538-4357/ac1c77)
- Kowalski, M., Ackermann, M., & Bartos, I. 2025, The promise of deep-stacking for neutrino astronomy, arXiv e-prints, arXiv:2501.10213, doi: [10.48550/arXiv.2501.10213](https://doi.org/10.48550/arXiv.2501.10213)
- Kun, E., Bartos, I., Tjus, J. B., et al. 2024, Possible correlation between unabsorbed hard x rays and neutrinos in radio-loud and radio-quiet active galactic nuclei, *PhRvD*, 110, 123014, doi: [10.1103/PhysRevD.110.123014](https://doi.org/10.1103/PhysRevD.110.123014)
- Liu, T., Buchner, J., Nandra, K., et al. 2022, The eROSITA Final Equatorial-Depth Survey (eFEDS): The AGN Catalog and Its X-ray Spectral Properties, *Astronomy & Astrophysics*, 661, A5, doi: [10.1051/0004-6361/202141643](https://doi.org/10.1051/0004-6361/202141643)
- Manconi, S., Korsmeier, M., Donato, F., et al. 2020, Testing gamma-ray models of blazars in the extragalactic sky, *PhRvD*, 101, 103026, doi: [10.1103/PhysRevD.101.103026](https://doi.org/10.1103/PhysRevD.101.103026)
- Miller, K. A., & Stone, J. M. 2000, The Formation and Structure of a Strongly Magnetized Corona above a Weakly Magnetized Accretion Disk, *ApJ*, 534, 398, doi: [10.1086/308736](https://doi.org/10.1086/308736)

- Murase, K., Guetta, D., & Ahlers, M. 2016, Hidden Cosmic-Ray Accelerators as an Origin of TeV-PeV Cosmic Neutrinos, *PhRvL*, 116, 071101, doi: [10.1103/PhysRevLett.116.071101](https://doi.org/10.1103/PhysRevLett.116.071101)
- Murase, K., Inoue, Y., & Dermer, C. D. 2014, Diffuse neutrino intensity from the inner jets of active galactic nuclei: Impacts of external photon fields and the blazar sequence, *PhRvD*, 90, 023007, doi: [10.1103/PhysRevD.90.023007](https://doi.org/10.1103/PhysRevD.90.023007)
- Murase, K., Kimura, S. S., & Mészáros, P. 2020, Hidden Cores of Active Galactic Nuclei as the Origin of Medium-Energy Neutrinos: Critical Tests with the MeV Gamma-Ray Connection, *PhRvL*, 125, 011101, doi: [10.1103/PhysRevLett.125.011101](https://doi.org/10.1103/PhysRevLett.125.011101)
- Senno, N., Mészáros, P., Murase, K., Baerwald, P., & Rees, M. J. 2015, Extragalactic Star-forming Galaxies with Hypernovae and Supernovae as High-energy Neutrino and Gamma-ray Sources: the case of the 10 TeV Neutrino data, *ApJ*, 806, 24, doi: [10.1088/0004-637X/806/1/24](https://doi.org/10.1088/0004-637X/806/1/24)
- Sommani, G., Franckowiak, A., Lincetto, M., & Dettmar, R.-J. 2025, Two 100 TeV Neutrinos Coincident with the Seyfert Galaxy NGC 7469, *ApJ*, 981, 103, doi: [10.3847/1538-4357/adb031](https://doi.org/10.3847/1538-4357/adb031)
- Ueda, Y., Akiyama, M., Hasinger, G., Miyaji, T., & Watson, M. G. 2014, TOWARD THE STANDARD POPULATION SYNTHESIS MODEL OF THE X-RAY BACKGROUND: EVOLUTION OF X-RAY LUMINOSITY AND ABSORPTION FUNCTIONS OF ACTIVE GALACTIC NUCLEI INCLUDING COMPTON-THICK POPULATIONS, *The Astrophysical Journal*, 786, 104, doi: [10.1088/0004-637X/786/2/104](https://doi.org/10.1088/0004-637X/786/2/104)
- Wilks, S. S. 1938, The large-sample distribution of the likelihood ratio for testing composite hypotheses, *Annals of Mathematical Statistics*, 9, 60, doi: [10.1214/aoms/1177732360](https://doi.org/10.1214/aoms/1177732360)
- Willox, E., & HAWC Collaboration. 2022, HAWC Follow-up on IceCube evidence from NGC 1068, *The Astronomer's Telegram*, 15765, 1
- Ye, Z. P., Hu, F., Tian, W., et al. 2023, A multi-cubic-kilometre neutrino telescope in the western Pacific Ocean, *Nature Astronomy*, 7, 1497, doi: [10.1038/s41550-023-02087-6](https://doi.org/10.1038/s41550-023-02087-6)
- Zegarelli, A., Franckowiak, A., Sommani, G., Valtonen-Mattila, N., & Yuan, T. 2025, IceCat-2: Updated IceCube Event Catalog of Alert Tracks, *arXiv e-prints*, arXiv:2507.06176, doi: [10.48550/arXiv.2507.06176](https://doi.org/10.48550/arXiv.2507.06176)
- Zhang, H., Cui, Y., Huang, Y., et al. 2025, A Proposed Deep Sea Neutrino Observatory in the Nanhai, *Astroparticle Physics*, 171, 103123, doi: [10.1016/j.astropartphys.2025.103123](https://doi.org/10.1016/j.astropartphys.2025.103123)
- Zhou, B., Kamionkowski, M., & Liang, Y.-f. 2021, Search for high-energy neutrino emission from radio-bright AGN, *PhRvD*, 103, 123018, doi: [10.1103/PhysRevD.103.123018](https://doi.org/10.1103/PhysRevD.103.123018)